Post-Selected Indistinguishable Photons from the Resonance Fluorescence of a Single Quantum Dot in a Microcavity

S. Ates,[1] S. M. Ulrich,[1] S. Reitzenstein,[2] A. Löffler,[2] A. Forchel,[2] and P. Michler[1]

[1]*Institut für Halbleiteroptik und Funktionelle Grenzflächen, Universität Stuttgart, Allmandring 3, 70569 Stuttgart, Germany*

[2]*Technische Physik, Universität Würzburg, Am Hubland, 97074 Würzburg, Germany*

(Received 20 May 2009; published 16 October 2009)

Applying continuous-wave pure resonant *s*-shell optical excitation of individual quantum dots in a high-quality micropillar cavity, we demonstrate the generation of post-selected indistinguishable photons in resonance fluorescence. Close to ideal visibility contrast of 90% is verified by polarization-dependent Hong-Ou-Mandel two-photon interference measurements. Furthermore, a strictly resonant continuous-wave excitation together with controlling the spontaneous emission lifetime of the single quantum dots via tunable emitter-mode coupling (Purcell) is proven as a versatile scheme to generate close to Fourier transform-limited ($T_2/(2T_1) = 0.91$) single photons even at 80% of the emission saturation level.

DOI: 10.1103/PhysRevLett.103.167402 PACS numbers: 78.67.Hc, 42.50.Dv, 42.50.St, 78.55.−m

Novel quantum information processing schemes like linear optics quantum computation and quantum teleportation are based on the effect of two-photon quantum interference [1] between single-photon pulses [2–6] on a beam splitter. An essential prerequisite for the successful realization of these applications is the possibility to generate indistinguishable photons. For pulsed operation, the two photons have to be Fourier-transform limited and identical in terms of pulse width, spectral bandwidth, carrier frequency, polarization, transverse mode profile, and arrival time at the beam splitter. The critical ingredient to create such 'ideal' photons is the initial excitation process of the emitter, which strongly influences the coherence properties and, consequently, the indistinguishability of the photons. So far, indistinguishability tests by two-photon interference have been reported from different model systems like single atoms [7], trapped ions [8], molecules [9], and semiconductor quantum dots (QDs) [10], all of which were subject to incoherent preparation of their corresponding radiative states.

Incoherent pumping of a solid-state single quantum emitter typically leads to homogeneous broadening of the excited state and therefore in a reduction in coherence time T_2. T_2 can be defined via the excited state's dephasing rate $T_2^{-1} = (2T_1)^{-1} + (T_2^*)^{-1}$, with T_1 as the radiative emitter lifetime and T_2^* as the pure dephasing time (coherence loss without recombination). Additionally, nonradiative relaxation from the excited to the emitting state introduces time jitter in the emission process. Recent investigations on single semiconductor QDs [11] explicitly revealed strong influence of incoherent optical excitation power on excitonic decay dynamics and two-photon interference, demonstrating reduced emission coherence and increased photon timing jitter as a consequence of enhanced multiexciton state formation. Theoretically [12], both the effects of pure dephasing and timing jitter should reduce the two-photon interference. Therefore, true resonant *s*-shell excitation appears crucial to generate indistinguishable photons. The challenge for resonant pumping in solid state is to separate the exciting laser light from resonantly scattered photons. Coherent excitation of a molecule emitting transform-limited photons was recently realized [13], but scattered laser background was of comparable magnitude as the fluorescence. True resonant *s*-shell excitation of a single QD was also demonstrated recently [14,15]. However, none of these papers presented two-photon interference measurements.

Our single-photon generation scheme is based on individual self-assembled (In, Ga)As/GaAs QDs embedded in a high-quality microcavity structure [16]. To ensure Fourier-transform-limited photon emission with negligible background we use an orthogonal excitation and detection technique [Fig. 1(a)]. We also benefit from the Purcell

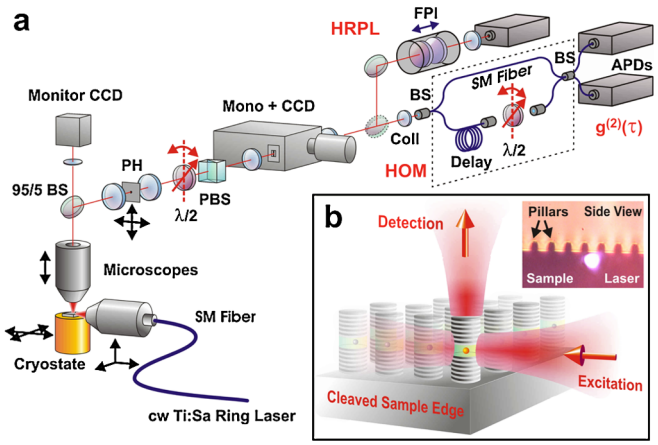

FIG. 1 (color online). (a) Experimental setups for low temperature micro-photo-luminescence (μ-PL), high-resolution PL (HRPL), and photon statistics (second-order correlation $g^{(2)}(\tau)$ and two-photon interference (HOM). [(P)BS: (polarizing) beamsplitter, FPI: Fabry-Pérot interferometer, PH: pinhole, SM: pol.-maintaining single-mode fiber, coll: collimator]. (b) Orthogonal excitation-detection geometry on individual micropillars; Inset: sideview of micropillars at the cleaved sample edge.

effect, leading to a reduction of T_1 and thus reducing the impact of possible phonon dephasing [17]. The efficient coupling of QD emission into the cavity mode and the enhanced photon collection from the microcavity serves to increase the signal-to-noise ratio as a key issue for high-visibility two-photon interference measurements. Single microcavities are optically addressed at the cleaved edges of our sample structure [Fig. 1(a) inset]. After spatial filtering of the collected micro-photoluminescence (μ-PL) by a pin-hole and spectral filtering by a monochromator, our setup provides high-resolution PL (HRPL; $\Delta E_{\mathrm{res}} = 0.7$ μeV) measurements by a scanning Fabry-Pérot interferometer (FPI) in combination with photon statistics in terms of $g^{(2)}(\tau)$ 2nd-order correlations [18] and two-photon interference.

Figure 2(a) shows a μ-PL spectrum of a 1.75 μm pillar cavity at $T = 10$ K under cw p-shell excitation. The PL peak at 1.357 eV is identified as the single neutral exciton recombination (X) whose fine-structure splitting becomes clearly visible in a Fabry-Pérot HRPL scan [Fig. 2(b)]. The fine-structure splitting is $\Delta E_{\mathrm{FS}} = 11.0 \pm 0.2$ μeV and the FWHM of the individual fine-structure components are 7.5 and 7.6 μeV, respectively. The fundamental mode (FM) of the cavity is mainly fed by nonresonantly coupled single excitonic emission [19–21] and some background contribution. By temperature tuning we are able to shift the X transition into resonance with the FM of the pillar cavity. This allows us to systematically decrease the radiative lifetime T_1 through the Purcell effect, and also enhance the photon collection efficiency. The resonance condition is reached at 24 K. Figure 2(c) shows the measured μ-PL decay times as a function of the QD-FM detuning ΔE. For this measurement, the sample was quasiresonantly excited (p shell) with 2 ps pulses of a mode-locked Ti:sapphire laser (76 MHz). Nearly symmetric in detuning around QD-mode resonance, a pronounced decrease of the decay time from 820 ± 10 ps at $\Delta E = 250$ μeV down to 65 ± 10 ps could be traced, reflecting a large Purcell factor ~13.

Figure 2(d) shows the result of a cw-laser (FWHM = 500 kHz) resonance scan (step width $\Delta f_{\mathrm{laser}} = 260$ MHz) over the X transition of the same single QD under synchronous emission detection. This signal, composed of QD resonance fluorescence and scattered laser light with a high signal-to-noise ratio ~5:1, reveals a well resolved double peak structure, which nicely reflects the fine-structure splitting ΔE_{FS} already measured in HRPL under p-shell excitation [Fig. 2(b)]. Despite a slightly increased sample temperature of 18 K we now obtain reduced FWHM values of the two components of only 6.1 ± 0.2 and 3.7 ± 0.2 μeV, respectively. This already indicates a reduced dephasing with respect to p-shell excitation. The occurrence of both fine-structure components in emission suggests a slight tilt of the main axes of the studied QD relative to the cleaved [110] sample edge. Otherwise, only one FS component could be excited with the horizontally polarized laser under side excitation. All subsequent measurements were performed under pure linearly polarized resonant excitation into the high-energy X component.

As was theoretically derived by Mollow [22], strong resonant excitation "dresses" a radiative two-level state into a quadruplet of two excited and two relaxed electronic states. Two of four resulting radiative transitions are spectrally degenerate at frequency $\omega_0 = \omega_{\mathrm{laser}}$ [Fig. 3(b)], and the original emission channel is characteristically decorated by spectral satellites $\omega_0 \pm \Omega$ (Ω: Rabi frequency).

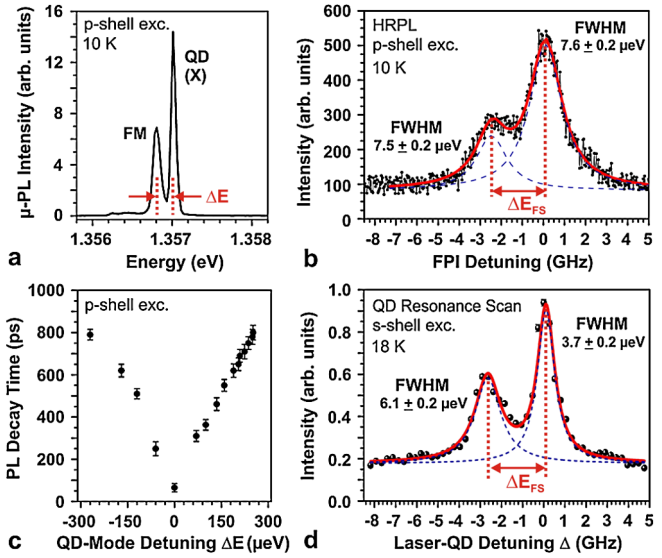

FIG. 2 (color online). (a) Low-temperature ($T = 10$ K) μ-PL spectra from the s shell of a single QD (excited via its p shell), showing emission close to a fundamental micropillar mode (FM). (b) High-resolution spectra of the same QD. (c) Excitonic luminescence decay time as a function of QD-FM detuning $\Delta E(T)$. (d) Frequency scanning signal obtained from the narrow band cw-laser tuned over the s shell of the single QD in (a).

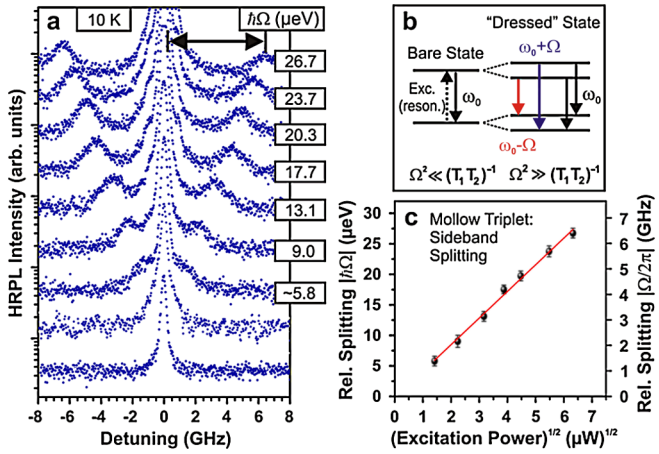

FIG. 3 (color online). (a) Power-dependent high-resolution PL (HRPL) spectra observed from a single QD under cw resonant s-shell excitation (log-scale). (b) Schematic of the evolution of a "dressed" state quadruplet with three nondegenerate transitions $\omega_0 \pm \Omega$ (Mollow-triplet) under strong resonant excitation, derived from the bare transition ω_0. (c) Excitation power-dependent Rabi splittings extracted from (a).

Observation of such "Mollow-triplet" signatures has recently been achieved from high-resolution laser absorption [23,24] and resonance fluorescence spectroscopy [15,25] on single QD structures. Figure 3(a) shows an excitation power-dependent Fabry-Pérot HRPL scan series of resonance fluorescence from the single QD in Fig. 2(a), observed at 10 K. According to theory [22], the central peak in a Mollow triplet includes two parts: i.e., an elastic coherent and an inelastic incoherent scattering component. The elastic component should dominate at very low power and exhibit a linewidth equal to that of the exciting cw laser (here: ~500 kHz). As this cannot be resolved within the spectral resolution (0.7 μeV) of our FPI, we expect a sum of a convoluted delta function (coherent part) and the incoherent contribution for the central peak. Our measured spectra display single Lorentzian line shapes in agreement with previous publications [14,25]. The width of the central resonance fluorescence peak depends on the Rabi energy Ω, T_1, and T_2, according to FWHM $= 2/T_2\sqrt{1 + T_1T_2\Omega^2}$ (see [14,25,26]). For low excitation $\Omega^2 \ll (T_1T_2)^{-1}$, the FWHM approaches $2/T_2$. For this low power limit, we can deduce a long coherence time of $T_2 = 1150 \pm 50$ ps from the experimentally observed linewidth of 1.15 ± 0.05 μeV in Fig. 3(a) (bottom trace). Notably, under these conditions the FWHM is found to be reduced by a factor of ~7 compared to the emission under p-shell excitation at the same temperature [10 K; Fig. 2(b)]. This demonstrates a pronounced reduction of dephasing processes achievable under resonant s-shell excitation and low T. Referring to a PL decay time of 630 ± 20 ps from our time-resolved measurements in Fig. 2(c) as T_1, we can infer a $T_2/(2T_1)$ ratio of 0.91 ± 0.05 under cw excitation conditions. Worth noting, the "true" lifetime T_1 should be slightly shorter than the measured decay time, thus creating a $T_2/(2T_1)$ ratio even closer to the ideal value of 1. This is because the nonradiative p-shell to s-shell ground state relaxation time (~10–50 ps) slightly increases the experimentally measured effective decay time with respect to T_1. We therefore conclude, that close to ideally Fourier-transform-limited single photons with >90% fidelity have been generated under resonant cw excitation.

Under increasing excitation powers, symmetric satellite peaks with increasing energy separation appear in the resonant QD emission spectrum [Fig. 3(a)]. A large Rabi splitting between these side and central peaks of $\hbar\Omega = 26.7$ μeV ($\Omega/2\pi = 6.4$ GHz) is obtained, being about a factor of 2 larger than corresponding values recently reported [15]. The side-to-central peak separation as a function of the effective Rabi frequency (proportional to the square-root of excitation power) reveals an almost perfect proportionality in accordance with the original theory [22] [Fig. 3(c)].

Second-order autocorrelation measurements performed at cw low-power resonant excitation conditions (~80% saturation level) revealed pronounced antibunching with $g^{(2)}(0) = 0.19 \pm 0.03$ [Fig. 4(a)]. Deconvolution with the time resolution of our HBT setup ($\delta t = 400 \pm 10$ ps) yields $g^{(2)}(0) = 0.08 \pm 0.02$, demonstrating the nearly pure single-photon nature of the collected signal (background ~4%) at this excitation power regime.

The laser background contribution considerably increases with excitation power and finally dominates the central feature of the Mollow spectrum. This is due to the nonlinear absorption of a resonantly excited two-level system (QD) which results in fluorescence emission saturation, while the laser signal increases linearly with power. For the photon correlation measurements in Fig. 4(a) as well as two-photon interference measurements discussed below, we therefore chose a low excitation power according to $\hbar\Omega \sim 0.9$ μeV (i.e., ~80% of the saturation level). In addition, the signal-to-background ratio was improved by decreasing the QD-FM detuning and utilizing the increasing Purcell effect [see Fig. 1(c)] together with enhanced QD-mode coupling. Ideally, zero detuning, e.g., perfect matching of the QD and cavity mode should be chosen at low temperature ($T < 10$ K) to avoid phonon dephasing processes. Practically, this was not possible in our experiment due to the limited time resolution $\delta t = 400 \pm 10$ ps of our sensitive detectors and the respective temperature (~24 K) at zero detuning. Consequently, a detuning was chosen for which the measured T_1 and T_2 times were comparable to our detector time resolution. Since we controllably reduce the QD-FM detuning by a slight temperature increase, the T_2 time decreases at the same time due to an increased phonon dephasing. We selected an intermediate QD-FM detuning of $\Delta E = 190$ μeV (with $T_1 = 560 \pm 20$ ps) where a linewidth measurement in the low intensity limit [Fig. 2(d)] yields a

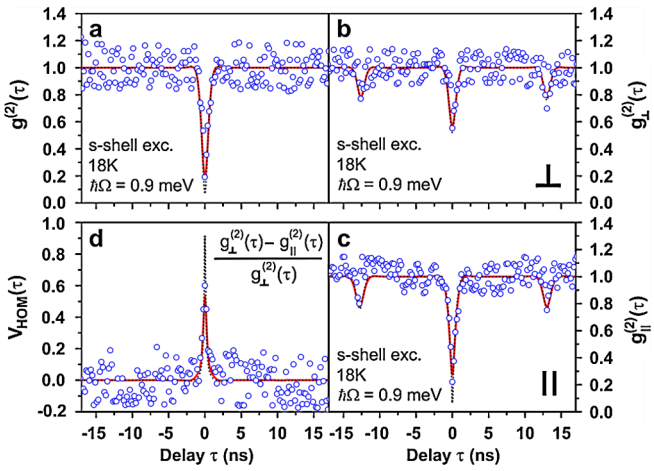

FIG. 4 (color online). (a) 2nd-order correlation measurement under low-power resonant QD s-shell excitation (18 K): $g^{(2)}(0) = 0.08$ (deconvoluted) reflects almost background-free single-photon emission. (b, c) Two-photon interference data under orthogonal and parallel polarizations of the interferometer arms, respectively. (d) Interference visibility obtained from traces (b) and (c). Solid lines (red) in all figures: Theoretical fits convolved with the system response ($\delta t = 400 \pm 10$ ps); dotted lines: deconvolved fits, i.e., corrected for δt.

FWHM of 3.7 μeV ($T = 18$ K), corresponding to $T_2 = 360$ ps. With this we achieve a signal-to-background ratio of ~20:1. The chosen detuning leads to a reduction of $T_2/(2T_1)$ to 0.32. However, this does not influence the principally measurable visibility of cw two-photon interference experiments (discussed below) since here the maximum observable visibility is given by the ratio $T_2/(2\delta t)$ (δt: detector response time) [27].

Hong-Ou-Mandel-type [1] two-photon interference measurements under resonant cw excitation were carried out with the asymmetric fiber-based Mach-Zehnder interferometer of Fig. 1(a). Figures 4(b) and 4(c) depict the results of the cw two-photon interference measurements $g_{\perp}^{(2)}(\tau)$ and $g_{\parallel}^{(2)}(\tau)$, describing correlations between photons with orthogonal and parallel polarizations, respectively. In orthogonal configuration, the two paths are distinguishable and one expects $g_{\perp}^{(2)}(0) = 0.5$, whereas in the parallel configuration the paths are indistinguishable and $g_{\parallel}^{(2)}(0)$ should ideally become zero [9,27]. We observe a value of $g_{\perp}^{(2)}(0) = 0.55 \pm 0.01$ and $g_{\parallel}^{(2)}(0) = 0.22 \pm 0.01$ for the orthogonal and parallel cases, respectively. In addition, two nearly equal correlation dips down to ~0.75 are observed at $\tau = \pm 13$ ns, thus indicating a balanced beam splitter. These dips reflect the chosen fixed path delay between the asymmetric interferometer arms [Fig. 1(a)] in cw measurements. The two-photon interference visibility can be defined [9,27] as $V_{\mathrm{HOM}}(\tau) = [g_{\perp}^{(2)}(\tau) - g_{\parallel}^{(2)}(\tau)]/g_{\perp}^{(2)}(\tau)$. Figure 4(d) shows the visibility curve with a maximum normalized value of 0.6 (convoluted with δt) at $\tau = 0$. In the following we analyze and discuss the results of the photon correlation measurements.

In a two-level coherent excitation the second-order coherence function $g^{(2)}(\tau)$ is determined by both T_1 and T_2 [13,28]. Taking the analytical formula for $g_{\perp}^{(2)}(\tau)$ and $g_{\parallel}^{(2)}(\tau)$ [27], the independently measured T_1 and T_2 times, and a convolution of the curves with our system response function, an excellent modelling (red curves) of all curves in Fig. 4 is obtained simultaneously. With this we find deconvoluted values of $g^{(2)}(0) = 0.08 \pm 0.02$, $g_{\perp}^{(2)}(0) = 0.53 \pm 0.03$, $g_{\parallel}^{(2)}(0) = 0.06 \pm 0.02$, and a visibility of $V_{\mathrm{HOM}}(0) = 0.90 \pm 0.05$, respectively. This large visibility value of ~90% demonstrates a high degree of postselective indistinguishability of photons within their coherence time and a nearly perfect overlap of the wave functions. Our results show the high potential of resonance fluorescence since the QD can be excited close to saturation without introducing significant dephasing. Thus, long coherence times T_2 and large values of $T_2/(2T_1)$ are possible for the generation of post-selected indistinguishable photons. We envision that the experiments can be extended to include a pulsed excitation scheme by using π-pulses to exactly excite one bright exciton state per pump cycle. In this scenario, the π-pulse spectral width has to be well matched to the linewidth of QD absorption in order to optimize the coherent excitation process and to minimize laser scattering. Prepared by such resonant triggered pumping conditions the QD will deterministically provide indistinguishable single photons with minimum timing jitter. With the presented QD-microcavity structures, Fourier-transform-limited single-photon generation at repetition rates well inside the GHz regime is anticipated.

In summary, our research highlights that the resonance fluorescence from a single semiconductor quantum dot in a micropillar cavity is a source of nearly ideal single photons even close to the saturation level of the QD. This type of single-photon generation is of direct interest for several applications in quantum information science, e.g., entanglement swapping [29].

We thank A. Kiraz for fruitful discussions, A. Wolf and M. Emmerling for their efforts to realize high-quality cleaved sample structures, as well as A. Ulhaq for supplementary measurements. We gratefully acknowledge financial support of the DFG via the research group "Quantum optics in semiconductor nanostructures."

[1] C. K. Hong *et al.*, Phys. Rev. Lett. **59**, 2044 (1987).
[2] B. Lounis and M. Orrit, Rep. Prog. Phys. **68**, 1129 (2005).
[3] M. Oxborrow and A. G. Sinclair, Contemp. Phys. **46**, 173 (2005).
[4] P. Michler *et al.*, Science **290**, 2282 (2000).
[5] B. Lounis and W. E. Moerner, Nature (London) **407**, 491 (2000).
[6] Z. Yuan *et al.*, Science **295**, 102 (2002).
[7] J. Beugnon *et al.*, Nature (London) **440**, 779 (2006).
[8] P. Maunz *et al.*, Nature Phys. **3**, 538 (2007).
[9] A. Kiraz *et al.*, Phys. Rev. Lett. **94**, 223602 (2005).
[10] C. Santori *et al.*, Nature (London) **419**, 594 (2002).
[11] A. J. Bennett *et al.*, Opt. Express **13**, 7772 (2005).
[12] A. Kiraz *et al.*, Phys. Rev. A **69**, 032305 (2004).
[13] G. Wrigge *et al.*, Nature Phys. **4**, 60 (2008).
[14] A. Muller *et al.*, Phys. Rev. Lett. **99**, 187402 (2007).
[15] A. N. Vamivakas *et al.*, Nature Phys. **5**, 198 (2009).
[16] A. Löffler *et al.*, Appl. Phys. Lett. **86**, 111105 (2005).
[17] D. Birkedal *et al.*, Phys. Rev. Lett. **87**, 227401 (2001).
[18] R. Hafenbrak *et al.*, New J. Phys. **9**, 315 (2007).
[19] K. Hennessy *et al.*, Nature (London) **445**, 896 (2007).
[20] D. Press *et al.*, Phys. Rev. Lett. **98**, 117402 (2007).
[21] M. Kaniber *et al.*, Phys. Rev. B **77**, 161303(R) (2008).
[22] B. R. Mollow, Phys. Rev. **188**, 1969 (1969).
[23] Xiaodong Xu *et al.*, Science **317**, 929 (2007).
[24] B. D. Gerardot *et al.*, New J. Phys. **11**, 013028 (2009).
[25] E. B. Flagg *et al.*, Nature Phys. **5**, 203 (2009).
[26] L. Allen and J. H. Eberly, *Optical Resonance and Two-level Atoms* (Wiley, New York, 1975).
[27] R. B. Patel *et al.*, Phys. Rev. Lett. **100**, 207405 (2008).
[28] R. Loudon, *The Quantum Theory of Light* (Oxford University Press, New York, 2000).
[29] M. Halder *et al.*, Nature Phys. **3**, 692 (2007).